

Syntheses of high molecular mass polyglycolides via ring-opening polymerization with simultaneous polycondensation (ROPPOC) by means of tin and zinc catalysts

Hans R. Kricheldorf¹ | Steffen M. Weidner²  | Andreas Meyer³

¹Institut für Technische und Makromolekulare Chemie, Universität Hamburg, Hamburg, Germany

²BAM, Federal Institute of Materials Research and Testing, Berlin, Germany

³Institut für Physikalische Chemie der Universität, Universität Hamburg, Hamburg, Germany

Correspondence

Hans R. Kricheldorf, Institut für Technische und Makromolekulare Chemie, Universität Hamburg, Bundesstr. 45, D-20146 Hamburg, Germany.

Email: hkricheldorf@aol.de

Abstract

Glycolide was polymerized in bulk by means of four different ROPPOC catalysts: tin(II) 2-ethylhexanoate (SnOct₂), dibutyltin bis(pentafluoro-phenoxy) (BuSnOPF), zinc biscaproate (ZnCap), and zinc bis(pentafluoro-phenyl sulfide) (ZnSPF). The temperature was varied between 110 and 180°C and the time between 3 h and 7 days. For the few polyglycolides (PGAs) that were soluble extremely high molecular masses were obtained. The MALDI TOF mass spectra had all a low signal-to-noise ratio and displayed the peaks of cyclic PGAs with a “saw-tooth pattern” indicating formation of extended-ring crystallites in the mass range below m/z 2500. The shape of DSC curves varied considerably with catalyst and reaction conditions, whereas the long-distance values measured by SAXS were small and varied little with the polymerization conditions.

KEYWORDS

cyclization, glycolide, ring-opening polymerization, tin catalysts, zinc catalysts

1 | INTRODUCTION

Research interested in polyglycolide (PGA) was initiated, when members of American Cyanamide and of DuPont filed in 1952/53 patents describing syntheses and properties of this biodegradable polyester mentioning that polyglycolide may be useful for medical applications.¹⁻³ These first patents were followed by relatively slow but steady flow of further patents and academic research articles.⁴⁻²⁷ In 1968 American Cyanamide commercialized PGA fibers under the trade-mark “Dexon” for application as resorbable medical suture. A few years later Ethicon Inc (subsidiary of Johnson & Johnson) followed with the commercialization of a medical suture under the trademark “Vicryl.” This suture was based on a copolyester of glycolic and lactic acid containing more than

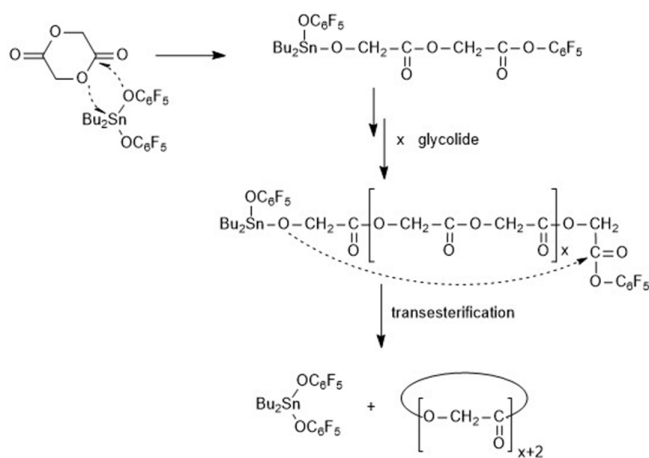
90% glycolic acid. These two medical sutures are still widely used in the 21st century. Further applications such as films for packaging purposes (trademark “Kuradex”) followed during the past 30 years.

PGA possesses a unique combination of properties. The lack of substituents allows PGA to form a compact crystal lattice by parallel arrangement of the linear chains in a planar *zick-zack* conformation, so that a kind of sheets is formed similar to that of the β -sheet structure of polyglycine. A consequence of this dense chain packing is a high density of crystalline PGA with a specific density that can reach values around 1.69 g cm^{-3} combined with a high hardness relative to that of other aliphatic polyesters.⁶ Another corollary is a stable crystal lattice with a high melting temperature (T_m up to 232°C)²⁰ and a high melting enthalpy (theoretical $\Delta H_m^0 = 206 \text{ J g}^{-1}$).¹⁴ The tight chain packing also entails excellent barrier properties against any kind of gases, in particular against non-polar gases. These barrier properties in combination

Dedicated to Professor Stanislaw Penczek on the occasion of his 90th birthday.

This is an open access article under the terms of the [Creative Commons Attribution-NonCommercial-NoDerivs](https://creativecommons.org/licenses/by-nc-nd/4.0/) License, which permits use and distribution in any medium, provided the original work is properly cited, the use is non-commercial and no modifications or adaptations are made.

© 2024 The Authors. *Polymers for Advanced Technologies* published by John Wiley & Sons Ltd.

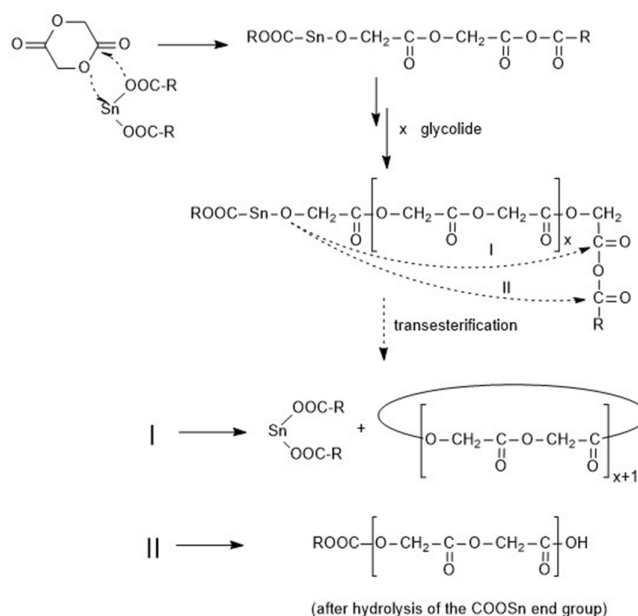


SCHEME 1 ROPPOC mechanism catalyzed by BuSnPhF.

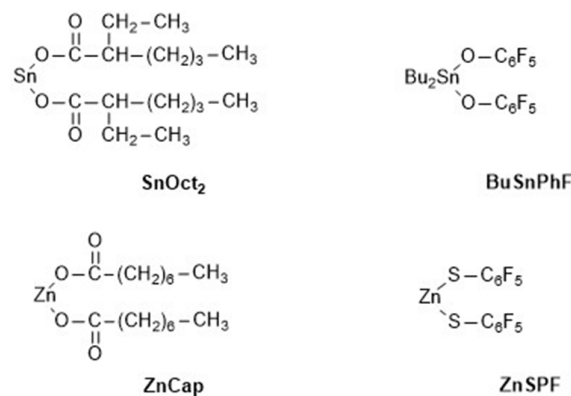
with a high mechanical strength renders PGA an interesting material for food packing. However, applications and research papers dealing with PGA remained scarce when compared with polylactide, because PGA also possesses a couple of negative properties. First, the polymerization of glycolide, which is the standard technical procedure, is highly exothermic and the heat flow is difficult to control when quantities of several tons are to be polymerized. Second, processing from the melt requires temperatures above 230°C which entail a high risk of thermal degradation with discoloration. Third, an inexpensive inert solvent has not been found yet, so that characterization in solution and processing from solution is hindered. The only solvent, which allows dissolution of low molecular mass PGA is hexafluoro-iso-propanol (HFIP), but high molecular PGA is insoluble even in this expensive solvent.

In the case of poly(L-lactide), PLA, the interest in cyclic PLAs has rapidly increased over the past 15 years, because the properties of cyclic polymers are in several aspects different from those of the corresponding linear polymers.²⁸ In the case of polar polyesters thermal processing may be easier and the thermal or hydrolytic stability higher than those of the linear polyesters. Furthermore, it has recently been found by the authors that crystallization and properties of the resulting crystallites may be different for cyclic and linear PLAs.^{29–32} For all these reasons the authors became interested in studying syntheses and properties of cyclic PGA, and in a recent publication the preparation of cyclic PGA via ring-expansion polymerization (REP) of glycolide was reported.³³ The present work has the purpose to explore the usefulness of ROPPOC catalysts (ROPPOC means ring-opening polymerization with simultaneous polycondensation and cyclization). The details of the ROPPOC mechanism depend on the nature of the catalyst. Metal phenoxides or phenyl sulfides initiate a relatively simple course as illustrated by Scheme 1.

The initiation step is followed by normal ring-opening polymerization via the coordination-insertion mechanism finally followed by end-to-end (ete) cyclization. In the case of PLA, cyclization was almost complete, when a reactive (electrophilic) CO end group was formed by a pentafluorophenoxide³⁴ or a pentafluoro-phenyl sulfide^{35,36} group. In the case of metal carboxylates, ete-cyclization (pathway I) competes with acylation of the Sn-O-alkyl end group (pathway II), which in turn yields linear chains with an acyl end group and a COOH



SCHEME 2 ROPPOC mechanism catalyzed by SnOct₂.



SCHEME 3 Structures and acronyms of the catalyst used in this work.

end group (Scheme 2). However, pathway II was found to be characteristic of tin(II) carboxylates at extremely high catalyst concentrations (monomer/catalyst ratios around 50/1 and below)^{37,38} but was not observed for Zn carboxylates.^{36,39} In this context, it was the purpose of this work to find out, if high molecular mass cyclic PGAs can be prepared by means of ROPPOC catalysts. In this connection it was the second purpose to compare the performance of tin and zinc catalysts. The chemical structures and acronyms of the catalysts used in this work are outlined in Scheme 3.

2 | EXPERIMENTAL

2.1 | Materials

Glycolide was purchased from Polyscience (Hirschberg, Germany) and recrystallized from anhydrous THF/toluene mixtures. Anhydrous THF

and toluene were purchased from Fisher Scientific (Schwerte, Germany). 1,4-Butane diol and diethylene glycol monomethyl ether were purchased from Sigma-Aldrich (Germany), dried azeotropically with toluene, distilled in vacuo and stored over mol-sieves. Tin(II) 2-ethylhexanoate (SnOct₂), purity >96% was purchased from Alfa Aesar (Kandel, Germany), and zinc caprylate (ZnCap) was purchased from MP Biochemicals. The catalysts dibutyltin bis(pentafluorophenoxide) (BuSnOPF) and zinc bis(pentafluorophenyl sulfide) (ZnSPF) were prepared as described previously.^{34,36}

2.2 | ROPs with neat catalysts

The catalyst (0.08 or 0.04 mmol) and glycolide (40 mmol) were weighed into a 50 mL flame-dried Erlenmeyer flask under a blanket of argon, and a magnetic bar was added. The reaction vessel was immersed into an oil bath thermostated at 140, 160 or 180°C. After cooling of the resulting PGA to ca. 25°C, the reaction vessel was destroyed and the solid disk of PGA was cracked into 4–6 pieces, which were used for annealing or for direct characterization.

The annealing was performed in an atmosphere of argon.

2.3 | Measurements

The MALDI TOF mass spectra were measured with Autoflex maX mass spectrometer (Bruker Daltonik GmbH, Bremen, Germany) equipped with a Smartbeam laser ($\lambda = 355$ nm). All spectra were recorded in the positive ion linear mode. The MALDI stainless steel targets were prepared from solutions of PGA in HFIP and doped with potassium trifluoroacetate (2 mg mL⁻¹). Typically, 20 μ L of sample the solution, 2 μ L of the potassium salt solution and 50 μ L of a solution of trans-2-[3-(4-tert-butylphenyl)-2-methyl-2-propenylidene] malononitrile (DCTB, 20 mg mL⁻¹ in HFIP) serving as matrix were mixed in an Eppendorf vial. 1 μ L of the corresponding solution was deposited on the MALDI target. FlexControl (Bruker Daltonik GmbH) was used to record spectra by accumulating 2000 single laser shots recorded at four different positions.

The GPC measurements were performed in a modular system kept at 30°C consisting of an isocratic pump (Agilent, USA) running with a flow rate of 0.5 mL min⁻¹ and a refractive index detector (RI-501-Shodex). HFIP was used as eluent. Samples were manually injected (100 μ L, ca. 2–4 mg mL⁻¹). For instrument control and data calculation WinGPC software (Polymer Standard Service-PSS now Agilent, Mainz, Germany) was used. The calibration was performed using a polymethylmethacrylate (PMMA) standard set (Polymer Standards Service—PSS, Mainz).

The DSC heating traces were recorded on a (with indium and zinc freshly calibrated) Mettler-Toledo DSC-1 equipped with Stare Software-11 using a heating rate of 10 K min⁻¹. Only the first heating traces were evaluated. The crystallinities were calculated with a ΔH_m max of -206 J g⁻¹.

The SAXS measurements were performed using our in-house SAXS/WAXS apparatus equipped with an Incoatec™ X ray source μ S and Quazar Montel optics. The wavelength of the X ray beam was 0.154 nm and the focal spot size at the sample position was 0.6 mm². The samples were measured in transmission geometry and were recorded with a Rayonix™ SX165 CCD-detector. The SAXS measurements were performed at sample-detector distance of 1.6 m and the accumulation was 1200 s. DPDACK, a customizable software for reduction and analysis of X-ray scattering data sets was used for gathering 1D scattering curves.⁴⁰ For the evaluation of the crystallinity of the samples the data were imported in Origin™ and analyzed with the curve fitting module. After subtracting of the instrumental background, the integral intensity of the crystalline reflections was divided by the overall integral intensity to determine the crystallinity. The SAXS curves were converted into Kratky plots. The long periods of the lamellar domains were determined by the q values of the reflection maxima.

3 | RESULTS AND DISCUSSION

3.1 | Polymerizations with tin catalysts

Polymerizations catalyzed by tin salts should be discussed first and the results obtained with BuSnOPF are presented prior to those obtained with SnOct₂, because of the simpler polymerization mechanism (Scheme 1).

It is well known that HFIP is the only relatively inert, low boiling liquid which can be used as solvent for the characterization of PGA by GPC or MALDI TOF mass spectrometry, but only the moiety of the 20 samples prepared in this work were completely soluble, although the solubility was tested with finely powdered samples at 50°C for 24 h. Therefore, only limited number average (M_n) and weight average (M_w) molecular masses data were accessible by GPC. These M_n and M_w values were unusually high, when compared to literature data. Yet, similarly high values were obtained in a recent study dealing with ring-expansion polymerization of glycolide.³³ M_n and M_w data reported previously for polylactides prepared via ring-expansion polymerization (REP) or with SnOct₂ and BuSnPhF were likewise high with M_n 's up to 200,000 and M_w 's up to 425,000.^{37,38}

From a review of this work and previous publications, the authors have learned that many polymer scientists expect the M_n of cyclic polyesters to be parallel to the monomer/initiator ratio. This expectation is not justified for the following reasons. For simplicity, a kinetic assumption based on three rate constants (k_{in} , k_{pr} , and k_{cy}) for initiation, propagation, and cyclization, should be considered. In the case of ROPPOC catalysts, the nucleophilicity of the initiator/catalyst is much lower than that of the metal alkoxide group forming the nucleophilic chain end. Therefore, the k_{pr}/k_{in} can be extremely high, and if the monomer is consumed before all the initiator/catalyst molecules have reacted, the resulting M_n 's exceed the theoretical one, as found in this study, where the theoretical M_n is 72,000 for a GL/cat ratio of 500/1.

When the cyclization is relatively fast and k_{pr}/k_{cy} and k_{pr}/k_{in} are relatively low, the resulting M_n 's are below the calculated ones, in as much as the initiator/catalyst liberated by fast cyclization may initiate

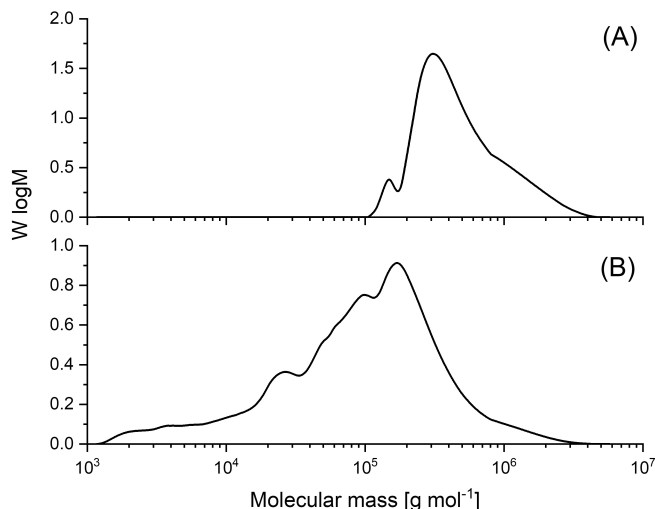


FIGURE 1 GPC elution curves of PGAs prepared in bulk with BuSnPhF at 180°C: (A) after 3 h (1A, Table 1) and (B) after 1 day (1B, Table 1).

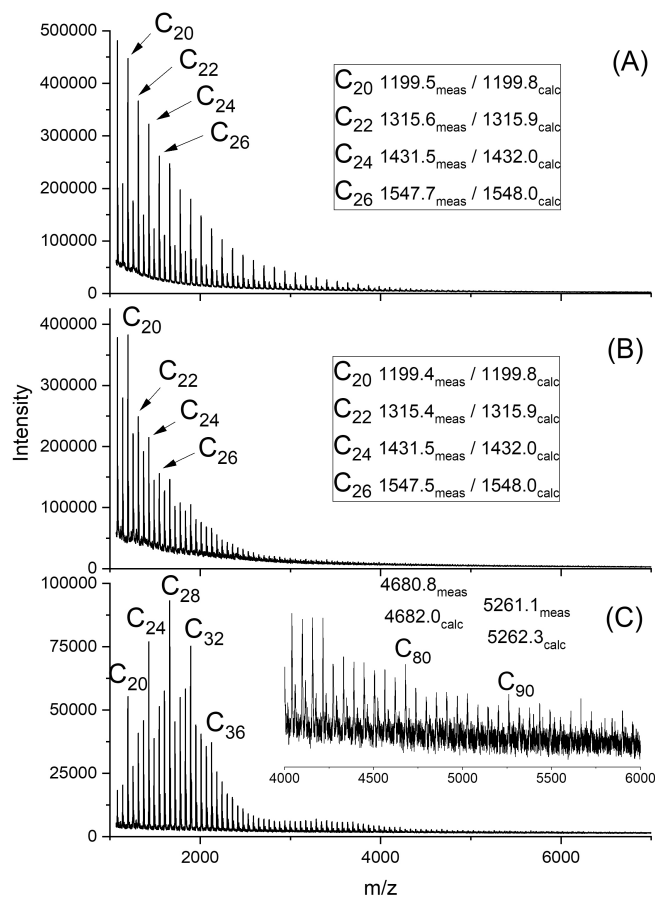


FIGURE 2 MALDI-TOF mass spectra of PGAs prepared with BuSnPhCl: (A) at 110°C/3 days (3A, Table 1), (B) 140°C/1 day (2A, Table 1), and (C) 180°C/1 day (1B, Table 1).

another chain, so that most initiators/catalysts initiated more than one chain. Therefore, M_n 's parallel to the monomer/initiator ratio are the exception and not the rule. Numerous papers by the author and other research groups describing syntheses of cyclic polyesters via ROPPOC (incl. zwitterionic polymerizations) or ring expansion polymerization support this conclusion.^{34,41-43}

The GPC elution curves of most PGA samples prepared in this work displayed shoulders, that indicate inhomogeneities in the mass distribution as illustrated in Figure 1. This result is not surprising, because PGA crystallizes extremely rapidly at all temperatures below 210°C, so that the polymerization kinetic is influenced by the crystallization, and the stirring of the melt may influence nucleation and orientation of the crystal growth.

For the MALDI TOF mass spectra of the PGAs prepared in this work only extremely low signal-to-noise ratios were achieved (Figures 2 and 3). Two reasons account for these poor spectra. First, the high molecular masses have the consequence that the fraction of PGA with masses below 15,000 Da which is needed for the MALDI TOF mass spectrometry is extremely low. This argument holds for any kind of polymer. However, the second reason is specific for PGA, namely the extraordinarily dense chain packing, due to the absence of substituents and a high concentration of polar groups along the chain, which entails strong electronic interactions between neighboring chains.

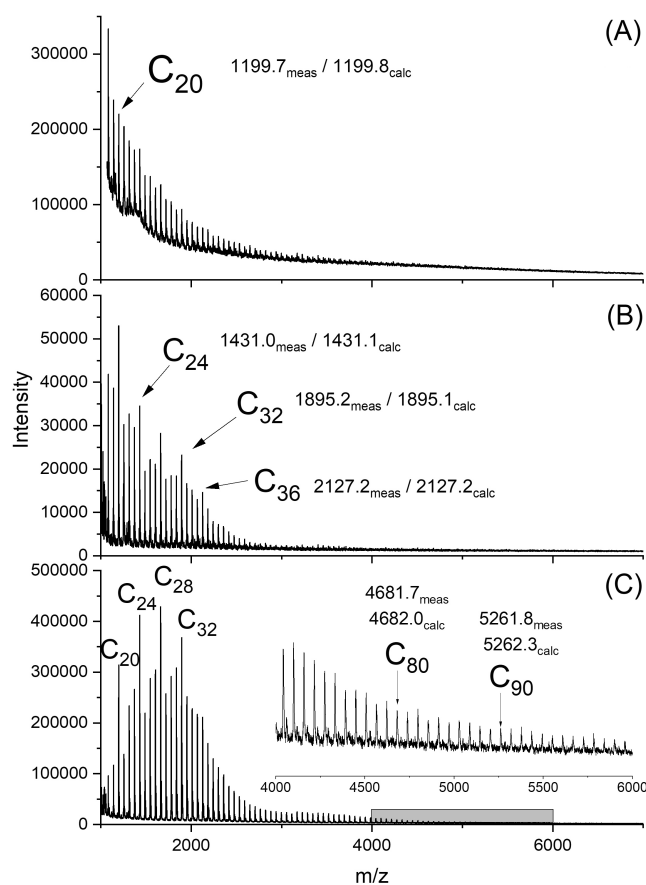
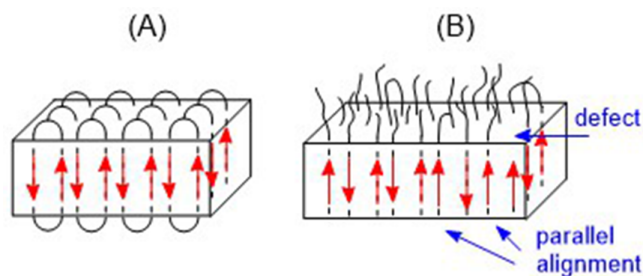


FIGURE 3 MALDI TOF mass spectra of PGAs prepared with SnOct₂: (A) at 110°C/3 days (3A, Table 2), (B) at 140°C/3 days (2A, Table 2), and (C) at 180°C/1 day (1B, Table 2).



SCHEME 4 2d-Illustration of a crystallite consisting of extended rings (A) or formed by rapid crystallization of linear chains (B).

Hence, PGA possesses a high specific weight (around 1.6 g/cm^3), and the highest melting point and highest melt enthalpy of all aliphatic polyesters.

A consequence of this dense chain packing is the difficulty to “evaporate” PGA chains by means of a laser beam. Therefore, the mass spectra displayed in Figures 2 and 3 represent the best examples obtained in this study. Nonetheless, these mass spectra carry two noteworthy pieces of information. First, only peaks of cycles are detectable. Second, these mass peaks display an unusual pattern, a kind of “saw-tooth pattern” (STP), which has recently been described for the first time by the authors for cyclic PLAs prepared via REP and ROPPOC.^{31,44} This STP is characteristic for annealed cyclic PGAs and PLAs having degrees of polymerization (DPs) below 100. Comparison of ring size with crystal thicknesses (as estimated from SAXS measurements) indicate that crystallites consisting of extended-cycles are formed (Scheme 4A), because their formation is kinetically and thermodynamically favored as discussed in several recent publications.^{31,44,45} Crystallites formed by linear chains of similar molecular masses have a higher tendency to include defects and they have a considerable disordered surface (Scheme 4B).

3.2 | Polymerizations with zinc catalysts

When ZSPF or ZnCa were used as catalysts, only three soluble PGA samples were found, but their molecular masses were nearly as high as those prepared with tin catalyst. Furthermore, mass spectra displaying peaks of cyclic PGAs with saw-tooth pattern were obtained, quite analogous to those displayed in Figures 2 and 3. Although peaks of cyclic PGAs were detected up to degrees of polymerization (DPs) around 90, these mass spectra do of course not prove that all the high molar mass chains also have a cyclic structure. In the case of REP the polymerization mechanism does not include an intermediate formation of linear species and a cyclic topology is a necessary consequence for low and high molar mass species. However, in the case of the ROPPOC mechanism, which is characteristic for the catalyst used in the present work (Schemes 1 and 2), linear chains are formed as the primary polymerization products, and it may happen that at least part of these linear chains are immobilized by crystallization prior to their cyclization. Therefore, the authors do not claim that their PGAs were

perfectly cyclic. However, it was recently learned from annealing of cyclic and linear poly(L-lactide)s in the presence of active polymerization/transesterification catalysts that various chain growth and cyclization reactions may proceed in the solid-state involving end groups and loops on the surface of the crystallites. Several transesterification reactions are outlined in the Schemes S1–S4 presented in the supplemental information (SI). Hence, it may be possible that chain growth reactions, ring expansion and cyclization reaction proceed even in the solid state. The high reactivity of the ester groups in PGA (when compared with polylactide) and the high temperatures certainly favor such transesterification reactions.

Finally, it should be emphasized that both Zn catalysts gave results, both in terms of molecular mass and MALDI mass spectra, that were comparable to those obtained with the tin catalysts used in this work. This finding was not expected based on previous studies with L-lactide, where the Zn catalyst proved to be significantly less reactive than the tin catalysts.^{36,39} The high reactivity of ZnCap at low temperatures (110°C , see below) is striking.

Finally, it should be mentioned that longer reaction times may result in a decrease of the molar masses. This phenomenon is well known from the polymerization of lactide catalyzed by tin catalysts, which is why a catalyst poison is added at the end of the polymerization in the technical production of polylactide. The main reason for the reduction of the initial M_n and M_w values is the ring-ring equilibration, because according to the Jacobson-Stockmayer theory⁴⁶ the M_n of equilibrated cycles is typically less than 5000 Da. The authors have recently⁴⁵ shown that ring-ring equilibration is also effective in the solid state for cyclic PLAs prepared by REP. Since the ester groups of PGA are more reactive than those of PLA I, it is not surprising that such degradation reactions also occur in solid PGA.

3.3 | DSC measurements

All DSC measurements were conducted with a heating rate of 10 K min^{-1} as usual for PGA and polylactide. Only the first heating trace was evaluated to avoid difficulties with thermal degradation, when samples heated to the molten state up to 260°C were cooled and heated a second time. Furthermore, the consequences of the annealing condition for melting temperature (T_m) and melting enthalpy (ΔH_m) should be studied. The DSC traces of the PGAs prepared with BuSnPhF, SnOct, and ZnSPF have several features in common. At the lowest temperature (110°C) and at the shortest reaction time (3 h) the DSC traces display a melting endotherm of unreacted glycolide as exemplarily illustrated in Figures 4A and 5A. Correspondingly, the ΔH_m values determined for the melting endotherm of PGA were low. These features were particularly pronounced for the ROP catalyzed with ZnSPF (Figure 5A), what means that this zinc salt showed the lowest activity of all four catalysts. After 7 h complete polymerization of glycolide was achieved and the ΔH_m values had significantly increased (Figures 4B and 5B and Tables 1–3). Under these conditions ZnCa proved to be the most active catalyst, and complete conversion of the monomer was achieved even within 3 h (Figure 6A).

Correspondingly, the crystallinity found after 3 h was nearly the same as that obtained after 7 h (Table 4).

In the DSC traces of all PGAs prepared at 140°C neither a melting endotherm of glycolide nor a glass-transition step of PGA was

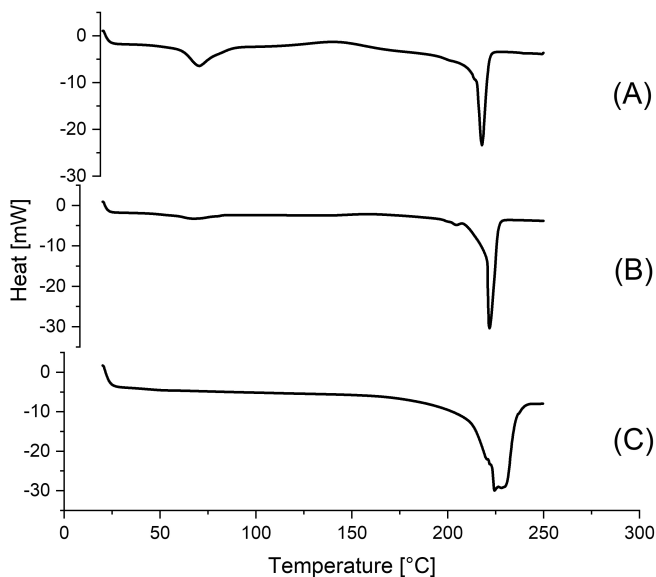


FIGURE 4 DSC heating traces of PGAs prepared with SnOct₂: (A) at 110°C/3 days (3A, Table 2), (B) at 110°C/7 days (3B, Table 2), and (C) at 140°C/1 day (2A, Table 2).

detectable (Figures 4C, 5C, and 6C). However, another interesting feature was found, namely the melting endotherms of the PGA displayed two peaks, presumably indicating two populations of crystallites with different perfection. This phenomenon was absent in the DSC traces of all PGAs, when the polymerizations were conducted at 180°C.

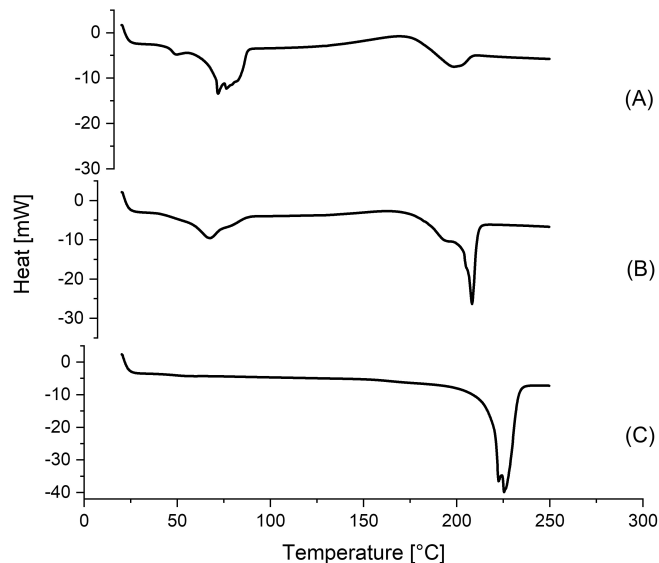


FIGURE 5 DSC heating traces of PGAs prepared with ZnSPF: (A) at 110°C/3 days, (B) at 110°C/7 days, and (C) 140°C/4 days.

TABLE 1 BuSnOPF-catalyzed polymerizations in bulk.

| Exp. no. | LA/Cat | Temp. (°C) | Time (d) | T_m (°C) | M_n | M_w | \bar{D} | ΔH_m (J g ⁻¹) | Cryst. (%) ^a | L (nm) |
|----------|--------|------------|----------|---------------|---------|----------------------|-----------|-----------------------------------|-------------------------|--------|
| 1A | 500/1 | 180 | 3 h | 223.8 | 370,000 | 600,000 | 1.6 | 119.6 | 58 | 7.4 |
| 1B | 500/1 | 180 | 1 | 222.9 | 310,000 | 190,000 | 6.1 | 131.5 | 64 | 7.1 |
| 2A | 500/1 | 140 | 1 | 227.4 | 210,000 | 360,000 | 1.7 | 111.4 | 54 | - |
| 2B | 500/1 | 140 | 4 | 224.5 | 145,000 | 425,000 | 2.9 | 117.2 | 57 | 7.2 |
| 3A | 500/1 | 110 | 3 | 211.0 | - | - | - | 64.4 | 31 | 7.6 |
| 3B | 500/1 | 110 | 7 | 222.6 + 226.1 | - | - | - | 106.3 | 51 | 6.4 |
| 4A | 100/1 | 160 | 1 | 223.9 | 420,000 | 710,000 ^b | 1.7 | 120.2 | 58 | - |
| 4B | 100/1 | 160 | 4 | 225.0 | - | - | - | 135.9 | 65 | - |

^aCalculated from DSC measurements with $\Delta H_m^0 = 206$ J g⁻¹.

^bRepetition of the ROP in 2 M o-dichlorobenzene gave $M_n = 355,000$, $M_w = 660,000$.

TABLE 2 SnOct₂-catalyzed polymerizations in bulk: GL/Cat = 500/1.

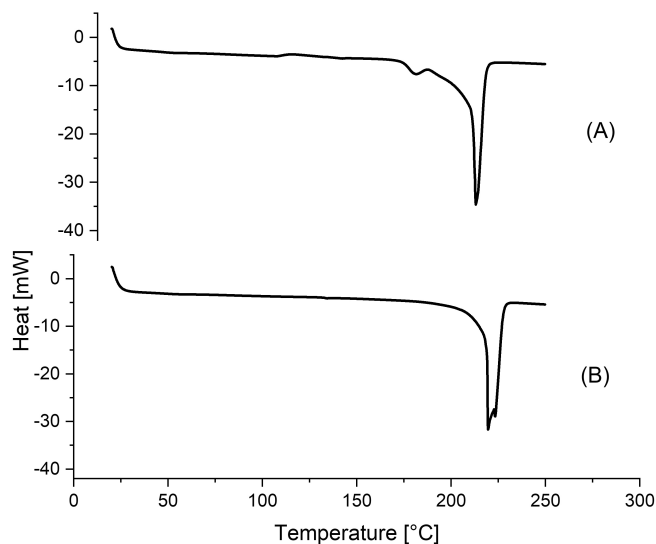
| Exp. no. | Temp. (°C) | Time (d) | T_m (°C) | M_n | M_w | \bar{D} | ΔH_m (J g ⁻¹) | Cryst. (%) ^a | L (nm) |
|----------|------------|----------|---------------|---------|---------|-----------|-----------------------------------|-------------------------|--------|
| 1A | 180 | 3 h | 224.3 | - | - | - | 117.7 | 56 | 7.6 |
| 1B | 180 | 1 | 222.9 | - | - | - | 121.8 | 58 | 7.4 |
| 2A | 140 | 1 | 224.1 + 230.0 | - | - | - | 119.1 | 57 | - |
| 2B | 140 | 4 | 225.0 | 110,000 | 310,000 | 2.8 | 121.6 | 58 | 7.1 |
| 3A | 110 | 3 | 217.2 | - | - | - | 78.8 | 38 | 7.5 |
| 3B | 110 | 7 | 221.2 | - | - | - | 96.2 | 46 | 7.4 |

^aCalculated from ΔH_m with $\Delta H_m^0 = 206$ J g⁻¹.

TABLE 3 ZnSPF-catalyzed polymerizations in bulk: GL/Cat = 500/1.

| Exp. no. | Temp. (°C) | Time (h) | T_m (°C) | M_n | M_w | \bar{D} | ΔH_m (J g ⁻¹) | Cryst (%) ^a | L (nm) |
|----------|------------|----------|---------------|---------|---------|-----------|-----------------------------------|------------------------|----------|
| 1A | 180 | 3 h | 226.1 | - | - | - | 114.1 | 55 | 8.0 |
| 1B | 180 | 1 | 222.7 | 144,000 | 330,000 | 2.3 | 129.0 | 62 | 7.7 |
| 2A | 140 | 1 | 223.3 | - | - | - | 120.2 | 58 | - |
| 2B | 140 | 4 | 221.0 + 225.4 | - | - | - | 119.4 | 57 | 7.3 |
| 3A | 110 | 3 | 198.3 | - | - | - | 14.2 | - | 7.7 |
| 3B | 110 | 7 | 208.1 | - | - | - | 64.4 | 31 | 8.4 |

^aCalculated from ΔH_m with $\Delta H_m^0 = 206 \text{ J g}^{-1}$.

**FIGURE 6** DSC heating traces of PGAs prepared with ZnCap: (A) at 110°C/3 days and (B) 140°C/4 days.

Another unexpected phenomenon was observed in the DSC traces of the PGAs prepared with ZnSPF and ZnCa at 180°C. When the PGAs were isolated after 3 h a weak glass transition step was observable in the temperature range of 176–180°C (Figure 7A,B). This glass-transition vanished upon annealing for 1 day. Such a high T_g is, at first glance, unlikely for an aliphatic polyester, in as much as the normal T_g of PGA falls into the range of 35–45°C, and one might be inclined to interpret this feature as a melting endotherm of less perfect crystallites. However, the same phenomenon at exactly the same temperature was observed for PGAs prepared via ring-expansion polymerization with cyclic tin catalysts under different conditions. In the case of the REP experiments, the glass-transition step appeared after annealing at 160°C for more than 1 day and vanished upon heating to 180°C for 1 day. The only fraction of PGA, which might be responsible for this phenomenon is the disordered immobile “phase” on the flat surfaces of the crystallites, but a straightforward explanation of this phenomenon cannot be forwarded at this time and requires more detailed studies.

Finally, the crystallinities calculated from the ΔH_m values need discussion. The calculation of crystallinities from ΔH_m measurements requires the knowledge of ΔH_m^0 , the maximum value of a perfect

crystal. Unfortunately, an absolutely reliable ΔH_m^0 of PGA has not been published yet. A ΔH_m of 139.7 J g⁻¹ was mentioned in the publications of Shawe et al.¹⁵ and of Nakka et al.,¹⁸ extracted from a Handbook of Polymer properties. However, this value is much too low as demonstrated by the experimental ΔH_m values published by Ayyoob et al.²⁰ and by the ΔH_m values presented in this work. More recently, a considerably higher value of 206 J g⁻¹ was mentioned by Ayyoob et al.²⁰ and Ramdanie et al.¹⁴ Yet, this value was calculated from one ΔH_m value and one crystallinity value given in a data sheet of the manufacturer of the “DEXON” fiber, and it is not clear, how the crystallinity of the DEXON fiber was determined. Nonetheless, a ΔH_m of 206 J g⁻¹ seems reasonable, since the crystallinities calculated with this value roughly agree with crystallinities (53%–63%) determined by Yu et al.¹⁹ via WAXS for a series of PGAs crystallized at different temperatures.

In summary, the DSC traces of the PGAs prepared in this work were considerably more informative than a simple listing of T_m values published in the literature let expect. This comment also considers the fact that almost all the DSC Figures of PGAs displayed in previous publications of other research groups show uniform monomodal heating traces.

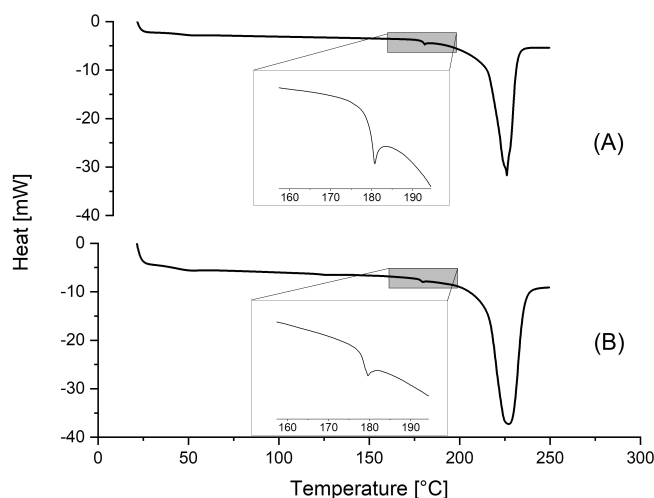
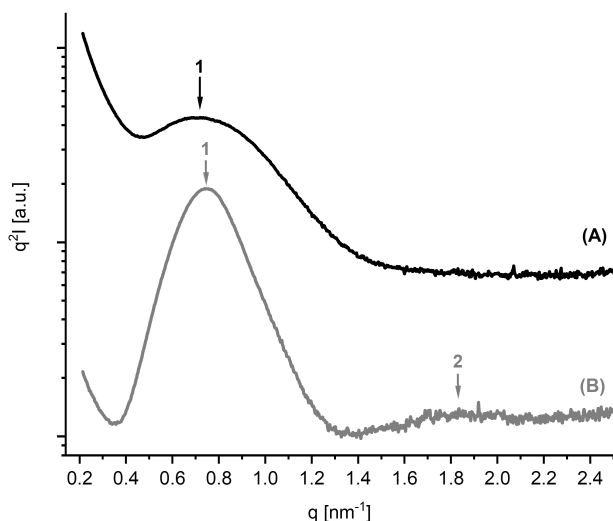
3.4 | SAXS measurements

Very little is known about SAXS measurements of PGAs, since long-distance (L) values have been reported in only two previous publications. Only a handful of L -values in the range of 6.2–7.6 nm were reported by Yu et al.¹⁹ The SAXS measurements of the present work gave the following results. The range of the L -values listed in Tables 1 and 2 perfectly agree with the literature data. In the case of PGAs prepared with Zn catalysts three values were slightly higher falling into the range of 8.0–8.4 nm. In the case of poly(L-lactide)s L -values in the range of 12–40 nm were reported. When compared with these PLA values it may be said that the L -values and thus, the crystal thickness of PGA crystallites are much smaller than those of poly(L-lactide) and the influence of catalysts and reaction conditions (annealing time and temperature) is considerably weaker. Two examples of SAXS measurements are presented in Figure 8 and in Figure S1 in the supplemental information (SI). Characteristic for all SAXS measurements is the finding that second order reflections are weak or absent,

TABLE 4 ZnCap-catalyzed polymerizations in bulk: GL/Cat = 500/1.

| Exp. no. | Temp. (°C) | Time (h) | T_m (°C) | M_n | M_w | \bar{D} | ΔH_m (J g ⁻¹) | Cryst (%) ^a | L (nm) |
|----------|------------|----------|---------------|---------|---------|-----------|-----------------------------------|------------------------|--------|
| 1A | 180 | 3 h | 227.2 | 410,000 | 630,000 | 1.5 | 98.2 | 47 | - |
| 1B | 180 | 1 | 225.3 | 147,000 | 338,000 | 2.3 | 129.4 | 63 | - |
| 2A | 140 | 1 | - | - | - | - | - | - | - |
| 2B | 140 | 4 | 220.2 + 225.4 | - | - | - | 99.5 | 48 | 8.1 |
| 3A | 110 | 3 | 213.0 | - | - | - | 113.8 | 55 | 8.5 |
| 3B | 110 | 7 | 214.1 | - | - | - | 114.8 | 56 | 6.2 |

^aCalculated from ΔH_m with $\Delta H_m^0 = 206 \text{ J g}^{-1}$.

**FIGURE 7** DSC heating traces of PGAs prepared at 160°C/3 h: (A) with ZnSPF (1A, Table 3) and (B) with ZnCap (1A, Table 4).**FIGURE 8** SAXS curves (Kratky plots) of PGAs prepared with ZnSPF: (A) at 110°C/7 days (3B, Table 3) and (B) at 180°C/3 h (Table 3).

indicating that the 3d-order of the crystallites inside the spherulites is poorly developed. A more detailed study of SAXS and WAXS measurements was not in the focus of the present work.

4 | CONCLUSIONS

The present work yielded a couple of unexpected results. First, that all the ROPPOC catalysts used in this work are efficient polymerization catalysts yielding high molecular mass PGAs. Second, tin and zinc catalysts showed a similar performance, whereas the zinc catalysts were considerably less active, when L-lactide was used as monomer. A third conclusion concerns the mass spectra which suggest that low molar mass cyclic PGA like low molar mass cyclic PLA has a high tendency to form extended-ring crystals with a thermodynamic controlled predominance of even-membered cycles. Fourth, the DSC measurements of samples prepared at 180°C and isolated after a few hours displayed a glass transition step around 175–180°C, which is quite unusual for an unsubstituted aliphatic polyester, and which defies a straightforward explanation at this time. In summary, it may be concluded that this work provides a stimulating basis for further studies of syntheses and properties of PGAs.

ACKNOWLEDGMENTS

We wish to thank the Federal Institute of Materials Research and Testing (BAM) for technical support and Dipl. Ing. A. Myxa (BAM) for the GPC measurements, and S. Bleck (TMC, Hamburg) for the DSC measurements. The authors would also like to thank Dr. S. Rost (Elantas/Altana SE, Hamburg) for kindly providing all the chemicals used in this work. Open Access funding enabled and organized by Projekt DEAL.

DATA AVAILABILITY STATEMENT

The data that support the findings of this study are available from the corresponding author upon reasonable request.

ORCID

Steffen M. Weidner  <https://orcid.org/0000-0001-8111-2765>

REFERENCES

1. US Pat., 2 585 427; 1952.
2. US Pat., 2 668 162; 1954.
3. US 2676945 Pat.; 1954.
4. Ishida Y, Ito H, Takayanagi M. Dielectric and viscoelastic behaviors of poly(hydroxyacetic ester). *J Polym Sci B Polym Lett*. 1965;3:87-94.
5. Chujo K, Kobayashi H, Suzuki J, Tokuhara S. Physical and chemical characteristics polyglycolide. *Die Makromol Chem*. 1967;100:267-270.

6. Chatani Y, Suehiro K, Ôkita Y, Tadokoro H, Chujo K. Structural studies of polyesters. I. Crystal structure of polyglycolide. *Die Makromol Chem*. 1968;113:215-229.
7. *US Pat., US 3 597449*; 1971.
8. *US Pat., 3 737 440*; 1973.
9. Gilding D, Reed A. Biodegradable polymers for use in surgery—polyglycolic/poly(actic acid) homo- and copolymers: 1. *Polymer*. 1979;20:1459-1464.
10. Chu C. Differential scanning calorimetric study of the crystallization kinetics of polyglycolic acid at high undercooling. *Polymer*. 1980;21:1480-1482.
11. Kister G, Cassanas G, Vert M. Morphology of poly(glycolic acid) by IR and Raman spectroscopies. *Spectrochim Acta A Mol Biomol Spectrosc*. 1997;53:1399-1403.
12. Dobrzynski P, Kasperczyk J, Bero M. Application of calcium acetylacetonate to the polymerization of glycolide and copolymerization of glycolide with ϵ -caprolactone and L-lactide. *Macromolecules*. 1999;32:4735-4737.
13. Amine H, Karima O, El Amine BM, Belbachir M, Meghabar R. Cationic ring opening polymerization of glycolide catalysed by a montmorillonite clay catalyst. *J Polym Res*. 2005;12:361-365.
14. Ramdhanie LI, Aubuchon SR, Boland ED, et al. Thermal and mechanical characterization of electrospun blends of poly(lactic acid) and poly(glycolic acid). *Polym J*. 2006;38:1137-1145.
15. Shawe S, Buchanan F, Harkin-Jones E, Farrar D. A study on the rate of degradation of the bioabsorbable polymer polyglycolic acid (PGA). *J Mater Sci*. 2006;41:4832-4838.
16. Gautier E, Fuertes P, Cassagnau P, Pascault JP, Fleury E. Synthesis and rheology of biodegradable poly(glycolic acid) prepared by melt ring-opening polymerization of glycolide. *J Polym Sci A Polym Chem*. 2009;47:1440-1449.
17. Schmidt C, Behl M, Lendlein A, Beuermann S. Synthesis of high molecular weight polyglycolide in supercritical carbon dioxide. *RSC Adv*. 2014;4:35099-35105.
18. Nakka RR, Thumu VR, Svs RR, Buddhiraju SR. The study of gamma irradiation effects on poly (glycolic acid). *Radiat Eff Def Solids*. 2015;170:439-450.
19. Yu C, Bao J, Xie Q, Shan G, Bao Y, Pan P. Crystallization behavior and crystalline structural changes of poly(glycolic acid) investigated via temperature-variable WAXD and FTIR analysis. *CrstEngComm*. 2016;18:7894-7902.
20. Ayyoob M, Lee DH, Kim JH, Nam SW, Kim YJ. Synthesis of poly(glycolic acids) via solution polycondensation and investigation of their thermal degradation behaviors. *Fibers Polym*. 2017;18:407-415.
21. Sanko V, Sahin I, Aydemir Sezer U, Sezer S. A versatile method for the synthesis of poly(glycolic acid): high solubility and tunable molecular weights. *Polym J*. 2019;51:637-647.
22. Shen K, Yang SL. Preparation of high-molecular-weight poly (glycolic acid) by direct melt polycondensation from glycolic acid. *Adv Mat Res*. 2013;821:1023-1026.
23. Pinkus A, Subramanyam R. New high-yield, one-step synthesis of polyglycolide from haloacetic acids. *J Polym Sci Polym Chem Ed*. 1984;22:1131-1140.
24. Schwarz K, Epple M. A detailed characterization of polyglycolide prepared by solid-state polycondensation reaction. *Macromol Chem Phys*. 1999;200:2221-2229.
25. Herzberg O, Gehrke R, Epple M. Combined in-situ small and wide-angle synchrotron x-ray scattering (SAXS-WAXS) applied to a solid-state polymerization reaction. *Polymer*. 1999;40:507-511.
26. Takahashi K, Taniguchi I, Miyamoto M, Kimura Y. Melt/solid polycondensation of glycolic acid to obtain high-molecular-weight poly(glycolic acid). *Polymer*. 2000;41:8725-8728.
27. Göktürk E, Pemba AG, Miller SA. Polyglycolic acid from the direct polymerization of renewable C1 feedstocks. *Polym Chem-Uk*. 2015;6:3918-3925.
28. Kricheldorf HR, Weidner S, Scheliga F. Cyclic poly(L-lactide)s via ring-expansion polymerizations catalysed by 2,2-dibutyl-2-stanna-1,3-dithiolane. *Polym Chem-Uk*. 2017;8:1589-1596.
29. Kricheldorf HR, Weidner SM, Meyer A. High Tm poly(L-lactide)s via REP or ROPPOC of L-lactide. *Polym Chem-Uk*. 2020;11:2182-2193.
30. Kricheldorf HR, Weidner SM, Meyer A. Poly(L-lactide): optimization of melting temperature and melting enthalpy and a comparison of linear and cyclic species. *Mater Adv*. 2022;3:1007-1016.
31. Kricheldorf HR, Weidner SM, Meyer A. Ring-expansion polymerization (REP) of L-lactide with cyclic tin catalysts—about formation of extended ring crystals and optimization of Tm and ΔH_m . *Polymer*. 2022;263:125516.
32. Kricheldorf HR, Weidner SM. About the crystallization of cyclic and linear poly(L-lactide)s in alcohol-initiated and Sn(II)2-ethylhexanoate-catalyzed ROPs of L-lactide conducted in solution. *Polymer*. 2023;276:125946.
33. Weidner SM, Meyer A, Kricheldorf HR. Cyclic polyglycolides via ring-expansion polymerization with cyclic tin catalysts. *Eur Polym J*. 2024;207:112811.
34. Kricheldorf HR, Weidner SM. Cyclic poly(L-lactide)s via simultaneous ROP and polycondensation (ROPPOC) catalyzed by dibutyltin phenoxides. *Eur Polym J*. 2018;109:360-366.
35. Kricheldorf HR, Weidner SM, Scheliga F. Cyclic polylactides via simultaneous ring-opening polymerization and polycondensation catalyzed by dibutyltin mercaptides. *J Polym Sci A Polym Chem*. 2017;55:3767-3775.
36. Kricheldorf HR, Scheliga F, Weidner SM. Syntheses of cyclic poly(L-lactide)s by means of zinc-based ring-opening polymerization with simultaneous polycondensation (ROPPOC) catalysts. *Macromol Chem Phys*. 2023;224:2300070.
37. Kricheldorf HR, Weidner SM. ROP of L-lactide and ϵ -caprolactone catalyzed by tin(ii) and tin(iv) acetates—switching from COOH terminated linear chains to cycles. *J Polym Sci*. 2021;59:439-450.
38. Kricheldorf HR, Weidner SM, Meyer A. About the influence of (non-) solvents on the ring expansion polymerization of L-lactide and the formation of extended ring crystals. *Macromol Chem Phys*. 2023;224:2200385.
39. Kricheldorf HR, Weidner SM, Scheliga F. Ring-opening polymerizations of L-lactide catalyzed by zinc caprylate: syntheses of cyclic and linear poly(L-lactide)s. *J Polym Sci*. 2022;60:3222-3231.
40. Benecke G, Wagermaier W, Li C, et al. A customizable software for fast reduction and analysis of large X-ray scattering data sets: applications of the new DPDPAK package to small-angle X-ray scattering and grazing-incidence small-angle X-ray scattering. *J Appl Cryst*. 2014;47:1797-1803.
41. Kricheldorf HR, Weidner SM. The ring-opening polymerization—polycondensation (ROPPOC) approach to cyclic polymers. *Macromol Rapid Commun*. 2020;41:e2000152.
42. Jeong W, Shin EJ, Culkin DA, Hedrick JL, Waymouth RM. Zwitterionic polymerization: a kinetic strategy for the controlled synthesis of cyclic polylactide. *J Am Chem Soc*. 2009;131:4884-4891.
43. Chang YA, Rudenko AE, Waymouth RM. Zwitterionic ring-opening polymerization of N-substituted eight-membered cyclic carbonates to generate cyclic poly(carbonate)s. *ACS Macro Lett*. 2016;5:1162-1166.
44. Weidner SM, Meyer A, Kricheldorf H. Sn(II)2-ethylhexanoate-catalyzed polymerizations of L-lactide in solution—solution grown crystals of cyclic poly(L-lactide)s. *Polymer*. 2022;255:125142.

45. Kricheldorf HR, Weidner SM. Ring-ring equilibration (RRE) of cyclic poly(L-lactide)s by means of cyclic tin catalysts. *Eur Polym J.* 2024; 206:112765.
46. Jacobson H, Stockmayer WH. Intramolecular reaction in polycondensations. I. The theory of linear systems. *J Chem Phys.* 1950;18:1600-1606.

SUPPORTING INFORMATION

Additional supporting information can be found online in the Supporting Information section at the end of this article.

How to cite this article: Kricheldorf HR, Weidner SM, Meyer A. Syntheses of high molecular mass polyglycolides via ring-opening polymerization with simultaneous polycondensation (ROPPOC) by means of tin and zinc catalysts. *Polym Adv Technol.* 2024;35(4):e6365. doi:[10.1002/pat.6365](https://doi.org/10.1002/pat.6365)